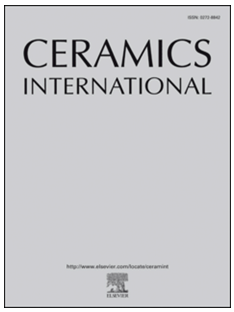

Fabrication of lanthanum-based perovskites membranes on porous alumina hollow fibre (AHF) substrates for oxygen enrichment

Ainun Sailah Sihar, Nur Hidayati Othman, Nur Hashimah Alias, Munawar Zaman Shahruddin, Syed Shatir Asghrar Syed-Hassan, Mukhlis A. Rahman, Ahmad Fauzi Ismail, Zhentao Wu

PII: S0272-8842(19)30797-7

DOI: https://doi.org/10.1016/j.ceramint.2019.03.242

Reference: CERI 21181

To appear in: *Ceramics International*

Received Date: 16 October 2018

Revised Date: 8 March 2019

Accepted Date: 30 March 2019

Please cite this article as: A.S. Sihar, N.H. Othman, N.H. Alias, M.Z. Shahruddin, S.S. Asghrar Syed-Hassan, M.A. Rahman, A.F. Ismail, Z. Wu, Fabrication of lanthanum-based perovskites membranes on porous alumina hollow fibre (AHF) substrates for oxygen enrichment, *Ceramics International* (2019), doi: https://doi.org/10.1016/j.ceramint.2019.03.242.

Fabrication of lanthanum-based perovskites membranes on porous alumina hollow fibre (AHF) substrates for oxygen enrichment

'Ainun Sailah Sihar[1], Nur Hidayati Othman[1]* , Nur Hashimah Alias[1], Munawar Zaman Shahruddin[1], Syed Shatir Asghrar Syed-Hassan[1], Mukhlis A. Rahman[2], Ahmad Fauzi Ismail[2],Zhentao Wu[3]

[1]Faculty of Chemical Engineering, Universiti Teknologi MARA, 40450, Shah Alam, Selangor.

[2]Advanced Membrane Technology Research Centre (AMTEC), Universiti Teknologi Malaysia, 81310 Johor Bahru, Johor.

[3]Aston Institute of Materials Research (AIMR), Aston University, Birmingham B4 7ET, UK

*Corresponding author: Email: nurhidayati0955@salam.uitm.edu.my

Tel.: +603 55448027; Fax: +603 55448301

Abstract-

In this work, two types of lanthanum-based MIEC perovskite oxides, namely $La_{0.6}Sr_{0.4}Co_{0.2}Fe_{0.8}O_{3-\delta}$ (LSCF) and $La_{0.6}Sr_{0.4}Co_{0.2}Ni_{0.8}O_{3-\delta}$ (LSCNi), were deposited onto porous alumina hollow fibre (AHF) substrates and used for oxygen enrichment. Such structure was developed to shorten oxygen ion diffusion distances in dense membranes and simultaneously leading to higher oxygen flux. The perovskite oxides were prepared using Pechini sol-gel method and deposited via a vacuum-assisted technique. The deposition of

lanthanum-based membranes onto the outer and inner sides of the porous AHF has been facilitated through numerous microchannels in the AHF substrates. The effects of operating temperature and argon sweep gas flowrate on oxygen permeation flux of lanthanum-based AHF membrane were investigated. The results revealed that the oxygen permeation flux of LSCF-AHF and LSCNi-AHF increased with operating temperatures due to the improvement of bulk diffusion and surface exchange properties after the lanthanum-based perovskite deposition. Higher oxygen flux was observed for LSCNi-AHF as LSCNi possessed balanced oxygen ionic and electronic conductivities as compared to LSCF membranes. Benefitting from improved oxygen activation and vacancy generation properties after Ni substitution into the B-site ion of LSC perovskite, a dramatic increased oxygen fluxes up to 4.5 mL/min·cm^2 was observed at 950 °C. The present work demonstrated a feasible method for fabricating oxygen transport membrane (OTM) using porous AHF substrates.

Keywords- *Alumina hollow fibre; MIEC perovskites; oxygen permeation; LSCF; oxygen enrichment*

1. Introduction

The market of oxygen production is rapidly expanding owing to their use in various industries such as metal production, petroleum refining, chemicals production, coal gasification and large-scale clean energy technologies[1]. There are two main technologies available for the separation of air, i.e cryogenic distillation and molecular sieve adsorbents via a process known as pressure swing adsorption (PSA). The selection of suitable technology is highly dependent on the scale of oxygen production, final purity and most

importantly, the cost. Currently, a low-temperature cryogenic distillation is preferred for applications that require tonnage quantities of oxygen, although it possess higher energy cost.

In recent years, development in mixed ionic electron conducting (MIEC) perovskite oxides and ceramic ionic transported membrane known as oxygen transport membrane (OTM) have attracted much attention and it is expected to replace the use of expensive cryogenic air separation. OTM derived from MIEC perovskite oxide shows enormous potential as it has infinite selectivity and good permeability towards oxygen separation/enrichment. The work was first initiated by Teraoka and co-workers [2–4] where they discovered MIEC material with perovskite structure namely $La_{1-x}Sr_xCo_{1-y}Fe_yO_{3-\delta}$ (LSCF) that has great potential for separating oxygen from air. Since then, MIEC perovskite compounds have been extensively studied and among them, LSCF is still considered as one of the most popular MIEC perovskites for various application such as cathodes in solid oxide fuel cell (SOFC) [5–7], membrane for partial oxidation of methane [8,9] and oxygen permeable membrane [10–12] owing to its good conductivity both, ionic and electronic [13]. In addition, LSCF also displays good chemical stability even under hydrogen atmosphere. However, it has relatively low oxygen permeability as compared to $Ba_{0.5}Sr_{0.5}Co_{0.8}Fe_{0.2}O_{3-\delta}$ (BSCF)[14]. In general, a number of factors can affects the oxygen permeation rate through a membrane such as operating temperature, sweep gas flowrate and compositions and most importantly, the membrane properties itself such as membrane materials, form, morphology and thickness [1,11,12,15–18]. Recently, LSCNi was investigated as a cathode materials for SOFC development [19] and oxygen sorbent [20]. It was found that better oxygen permeation can be achieved by substitution of Fe with Ni due to low polarization resistance. This leads to the increase of oxygen vacancies (δ) that is necessary for ionic conduction through the perovskite oxide materials.

The oxygen transport in OTM membrane is based on conventional molecular diffusion where oxygen molecules are first dissociated or deionized into its ion form in the crystal lattice [21]. The oxide ions are then transported through the dense MIEC perovskite membrane wall under gradient of oxygen partial pressure from high to low side. But, this mechanism requires high thermal energy for the oxygen ions to overcome the energy barrier to allow them to hop in the lattice and thus, associates back to form oxygen molecules at the permeate side of the membrane. As a result, the OTM always operated at elevated temperature (700-1200 °C).

Other factors that likely to limit the performance of the OTM are bulk diffusion of oxygen through membrane and surface exchange reaction. The bulk diffusion can be resolved by reducing the membrane thickness as the diffusion rate is the slowest step due to the thick membrane wall. However, the decrease of membrane thickness can also affected the mechanical strength and causing membrane failure during operation. Many works have been carried out in developing asymmetric supported OTM membranes where a thin dense transport layer is usually supported on a thick substrate. The used of thick substrate can helps in improving the mechanical strength of the membrane. By modifying the thick substrates to having porous structure, higher oxygen permeation can be expected due.

Kingsbury and Li [22] and Lee et. al [23–25] have successfully fabricated porous alumina hollow fibre substrates consisting of finger-like pores by varying the bore fluid and air gap distance used during the spinning process. The finger-like pores on the lumen side of the alumina hollow fibre substrate not only offers great surface area for surface exchange reaction to occur but can also reduce diffusion resistance during the oxygen permeation process [26,27]. The synthesis of MIEC perovskite oxides in bulk is quite tedious and therefore, it will be very costly to be used as substrate material. By thinly depositing the

perovskite oxides onto alumina hollow fibre (AHF) substrates, the fabrication cost of OTM can be minimized as well as enhancing the oxygen permeation fluxes.

Perovskite oxides can be synthesized using a number of methods such as sol-gel, combustion, co-precipitation and spray-pyrolysis. However, sol-gel method is more preferable due to its simplicity and low cost. The sol-gel method is divided into 2 types i.e. colloidal-sol and polymeric-sol [28]. Many studies preferred the use of Pechini-type polymeric precursor for thin film coating as compared to sol-gel alkoxide [29]. This is because sol–gel alkoxide precursors are quite sensitive in moisture and the film tends to crack during the drying process. As Pechini process use a polymeric precursor that consists of randomly macromolecular chains where the metal cations are uniformly distributed on an atomic level. Therefore, a uniform and homogeneous cation distribution can be achieved during the membrane deposition process. Dip-coating technique has been widely used for perovskite oxide deposition on the hollow fibre membrane surface [30–32]. In this technique, the membrane substrate was immersed into the coating sol to procure a uniform coating layer on both surface sides of the membrane. Recently, a new coating method where vacuum condition in introduced into the coating system was proposed [33,34]. The use of vacuum allows uniform coating inside the membrane microchannels by removing the air inside the hollow fibre prior to the introduction of coating solution. In this way, more perovskite oxide can be deposited while avoiding non-homogeneous and crack issues faced by the dip-coating method. In this work, we proposed a new method on the formation of thin lanthanum-based perovskite membranes (LSCF and LSCNi) onto porous AHF substrates for oxygen enrichment.

2. Experimental

2.1. Preparation of lanthanum-based perovskite sol-gel

The perovskite oxides were prepared using sol-gel method where metal nitrates were used as precursors. For the preparation of $La_{0.6}Sr_{0.4}Co_{0.2}Fe_{0.8}O_{3-\delta}$ (LSCF), stoichiometric amount of metal nitrates such as $La(NO_3)_3.6H_2O$, $Sr(NO_3)_2$, $Co(NO_3)_2.6H_2O$ and $Fe(NO_3)_3.9H_2O$ were first dissolved in distilled water. Anhydrous citric acid ($C_6H_8O_7$) and ethylene glycol ($C_2H_6O_2$) were then added to the metal nitrates solution with a molar ratio of ethylene glycol to citric acid to metal nitrates of 9:3:1. As the chelating effect is favored by the pH, adequate volumes of 10 % NH_3 were added into the solution in order to increase the pH value to 7. The solution was stirred and heated at 80 °C for 5 h until a brownish sol was formed. The calcination of sol was carried out at 850 °C for 4 h to form pure perovskite structure using heating rate of 2 °C/min. Similar method was used to prepare $La_{0.6}Sr_{0.4}Co_{0.2}Ni_{0.8}O_{3-\delta}$ (LSCNi) sol-gel using their metal nitrates. The flow of perovskite sol-gel synthesis is shown in Fig. 1.

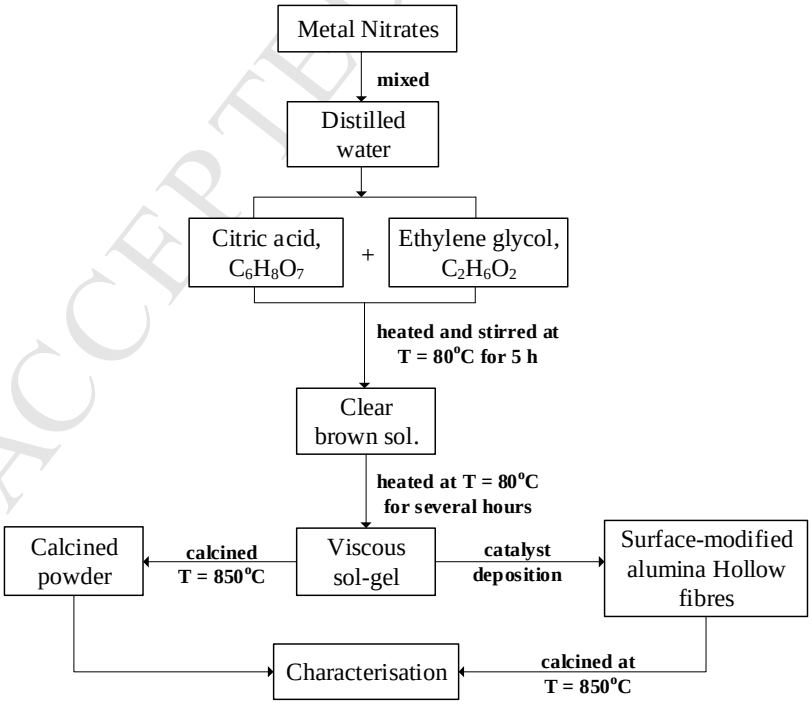

Fig. 1. Process flow diagram of preparation of MIEC perovskite

2.2. Fabrication of alumina hollow fibres

Alumina hollow fibre substrates were prepared using phase inversion/sintering technique with suspension composition of 55 wt% alumina powder (< 1.0 µm aluminium oxide, Alfa Aesar, UK), 0.38 wt% arlacel (Uniqema, USA), 39.12 wt% dimethyl sulfoxide (DMSO; VWR) and 5.5 wt% polyethersulfone (PESf Radal A300; Ameco Performance). Hexane and tap water were used as internal and external coagulants, respectively. The suspension mixture was extruded using a tube-in-orifice spinneret with the orifice diameter/inner diameter of 3.0/2.8 mm into the coagulation bath. The extrusion rate and internal coagulant flowrate were both controlled at 15 mL/min with zero air gap. Two step sintering process was carried out where the furnace temperature was first increased from room temperature to 600 °C at a rate of 2 °C/min and held for 2 h followed by an increment to 1450 °C at a rate of 5 °C/min and held for another 4 h before being cooled to room temperature.

2.3. Deposition of lanthanum-based perovskites on alumina hollow fibre substrates using vacuum-assisted technique

The prepared LSCF perovskite sol-gel was then deposited onto AHF by using vacuum-assisted technique to enhance the deposition of perovskite oxides into the pores [35,36]. The AHF was first vacuumed to remove the air inside the hollow fibre and the tube containing the bare fibres was then filled with perovskite sol-gel solution. The coating process was carried out under vacuum condition for one hour. The surface-modified AHF were dried in air for 24 h prior to the calcination process. The calcination was carried out at 850 °C for 4 h to remove organic binder and to form pure perovskite structures, followed by 1050 °C for another 2 h. A heating and cooling rate of 5 °C/min was used during this study. Similar steps were

adopted for LSCNi perovskite sol-gel and the amount of perovskite oxide deposited onto the fibre surface was then calculated using the equation below;

$$\text{Percentage of weight gain}, \% = \frac{W_2 - W_1}{W_1} \times 100 \quad (1)$$

where, W_1 is the initial weight of bare alumina fibre(g) and W_2 is the weight of surface-modified alumina fibres after calcination process (g).

2.4. Gas tightness and oxygen permeation study

Gas tightness and oxygen permeability of the LSCF-AHF and LSCNi-AHF membranes were evaluated using gas permeation setup shown in Fig. 2. The gas tightness test were conducted using nitrogen and low gas permeance (>1 x10^{-10} mol.m^{-2}.s^{-1}.Pa^{-1}) indicates that the membrane is gas-tight and can be used as OTM. The test gas was pressurised into the membrane sample by creating a sealed system. The pressure change with time was monitored and recorded. The gas permeance, P (mol.m^{-2}.s^{-1}.Pa^{-1}) was then calculated based on the change of pressure with time using the equation below:

$$P = \frac{V}{RTAt} ln\left(\frac{P_o}{P_t} - \frac{P_a}{P_a}\right) \quad (2)$$

$$A = \frac{\pi L\,(D_o - D_i)}{ln\frac{D_o}{D_i}} \quad (3)$$

where V is the volume of the test compartment (m^3); R is the gas constant (8.314 J.mol^{-1}.K^{-1}); t is the measurement time (s) and T is the measured temperature (K). P_0 and P_t are the initial and final measured pressures in the test cylinder (Pa); P_a is the atmospheric pressure (Pa). A is

the effective membrane area deposited with perovskites, D_o, D_i and L are the outer diameter, inner diameter and the effective length for oxygen permeation of the deposited hollow fibre membrane, respectively.

For oxygen permeation study, the AHF was attached to a dense mullite tube (od/id = 9/6 mm) and both ends of the fibre was sealed using high temperature sealant. The seal was verified as a gas-tight if nitrogen was not detected during the study. Permeation testing was conducted by passing argon as a sweep gas through the hollow fibre lumen side to collect the permeated oxygen. The flowrates of argon were controlled by mass flow controller, which were calibrated using bubble flowmeter. Oxygen permeation experiment was carried out by varying the sweep gas flowrates from 50 to 150 mL/min and operating temperature between 700 to 950 °C. The total flowrate of the permeate was measured using bubble flowmeter and the oxygen permeation flux is calculated using equation (4);

$$J_{O_2} = \left(x_{O_2} - \frac{21}{79} x_{N_2}\right) \times \frac{V}{A} \tag{4}$$

where x_{O_2} and x_{N_2} are the oxygen and nitrogen concentration in the effluent.

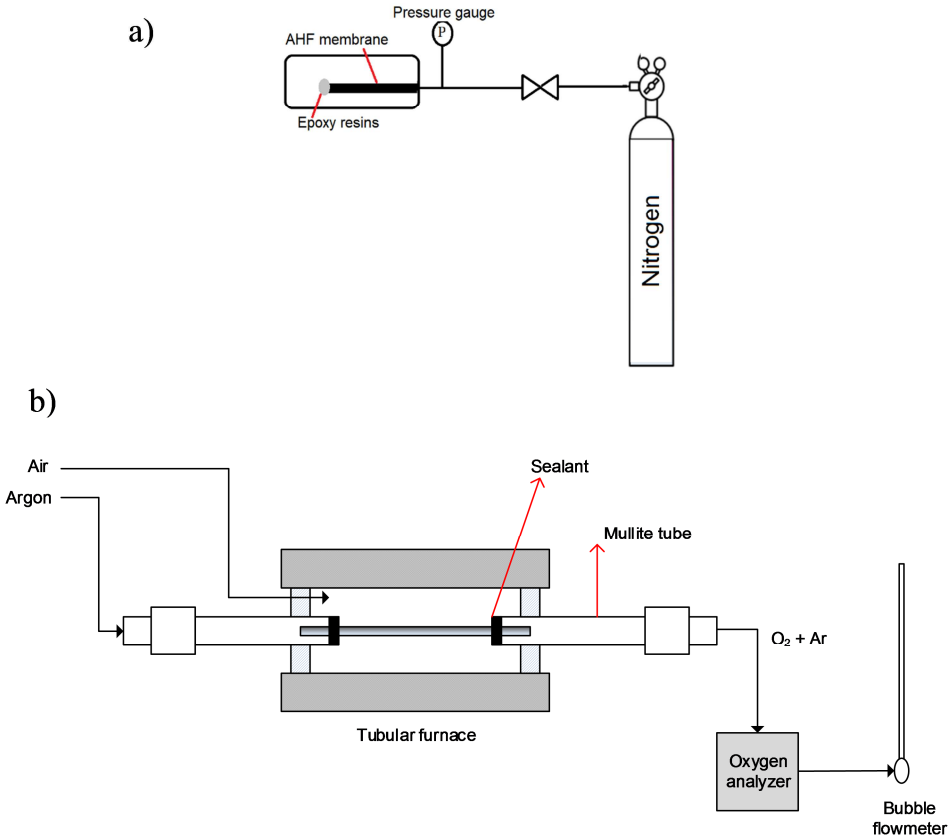

Fig. 2. Schematic diagram of experiment setup; (a) gas tightness and (b) oxygen permeation

2.5. Characterizations

The crystallite structure of perovskite oxides was analysed using X-ray diffractometer (XRD; D/Max 2200/PC, Rigaku, Japan) using Cu-Kα radiation source with scanning ranging from 10° to 80° at a rate of 5°/min. The voltage and current used for the scanning were 40 kV and 40 mA, respectively. The morphological study of the surface-modified hollow fibre membranes were observed using scanning electron microscopic (SEM; S-3400N, Hitachi, Japan) with energy dispersive spectroscopy (EDS) analysis (XFlash 610, Bruker, USA). The pore size distribution and porosity percentage of the bare and surface-modified membranes were analyzed using mercury porosimetry (IV 9510, Micromeritics Autopore, USA).

3. Results and Discussion

3.1. Perovskite characterizations

Fig. 3 depicts the XRD patterns of LSCF and LSCNi perovskite oxide. All the samples were prepared using sol-gel method and calcined at 850 °C for 4 hours. Both calcined powders show good formation of single-phase perovskite structure. Strong characteristic peaks of $La_{0.6}Sr_{0.4}Co_{0.2}Fe_{0.8}O_{3-\delta}$ were found at $2\theta_{110}$ = 32.58°, $2\theta_{202}$ = 40.0°, $2\theta_{024}$ = 46.8°, $2\theta_{214}$ = 58.22°, $2\theta_{208}$=68.38° and $2\theta_{218}$=77.6° [30]. Meanwhile, the characteristic peaks for $La_{0.6}Sr_{0.4}Co_{0.2}Ni_{0.8}O_{3-\delta}$, were observed at $2\theta_{110}$ = 32.94°, $2\theta_{202}$ = 40.64°, $2\theta_{024}$ = 47.34°, $2\theta_{214}$ = 58.7°, $2\theta_{208}$ = 69.2° and $2\theta_{218}$ = 78.84°. The peaks observed in LSCNi oxide were found to be consistent with the work reported by Hjalmarsson et. al [19]. This finding confirms that the Ni dopant ion has been successfully incorporated into the lattice host. The substitution of Ni into the B-site ion of perovskite also has caused the characteristic peaks to slightly shift to the right indicating a decreased in volume unit cell. This was because ionic radius of the doping ions, Ni^{2+}, is smaller than its substituting element (Co) of lattice $La_{0.6}Sr_{0.4}CoO_3$ oxide, which leads to the decreased of lattice parameter [4].

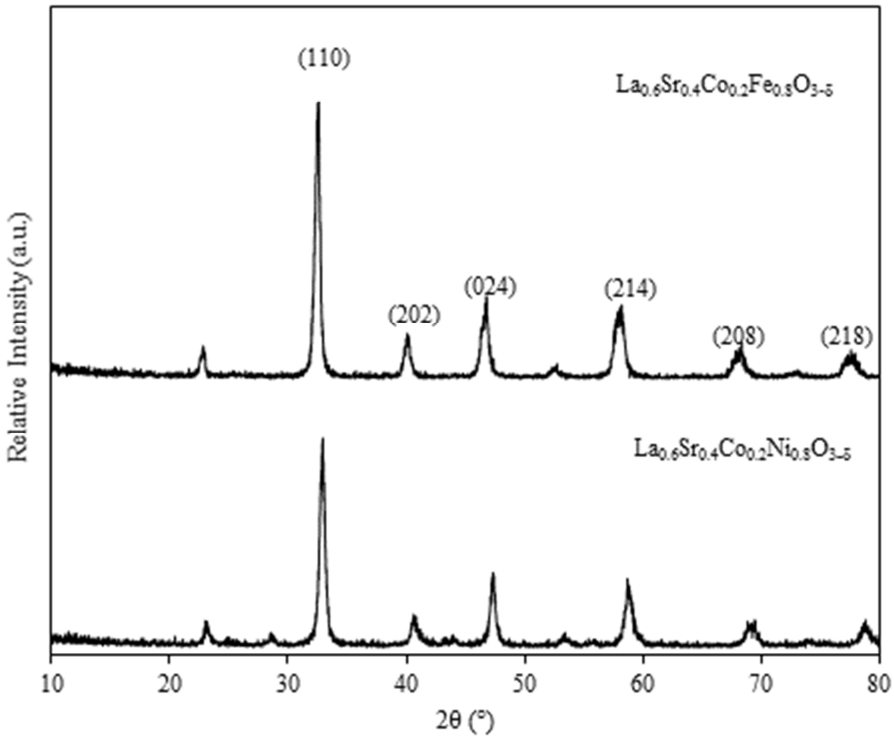

Fig. 3. X-ray diffraction patterns for the perovskite MIEC oxide catalysts calcined at 850 °C for 4 h

3.2 Morphology of the lanthanum-based surface-modified hollow fibre membranes

The morphology of bare AHF substrates sintered at 1450 °C is shown in Fig. 4. Sintering temperature has been known to significantly affect the properties of ceramic membranes particularly morphology, porosity and mechanical strength [36]. Higher sintering temperature could improve the membrane strength but at the same time the pores of membrane decreases, which could affect the deposition efficiency. From Fig. 4(a), the outer and inner diameter of the AHF was measured to be 2.16 and 1.67 mm giving a membrane thickness of 0.49 mm. The substrate was oin asymmetric structure contains a finger-like structure that was formed from the inner surface and sponge-like structure toward the outer surface. Small open pores at the inner surface of the hollow fibre substrate was observed and such structure was formed

due to the use of a mixture of n-hexane solvent in water. Besides, the use of air gap has led to the suppression of finger-like structure near to the outer surface and the viscous fingering may not occurs due to solidification of the outer surface of hollow fibre before the immersion into the external coagulation bath [37]. It is believed that the existence of the finger-like structure and open pores at the inner face could facilitate the deposition of MIEC perovskite sol on the AHF substrates.

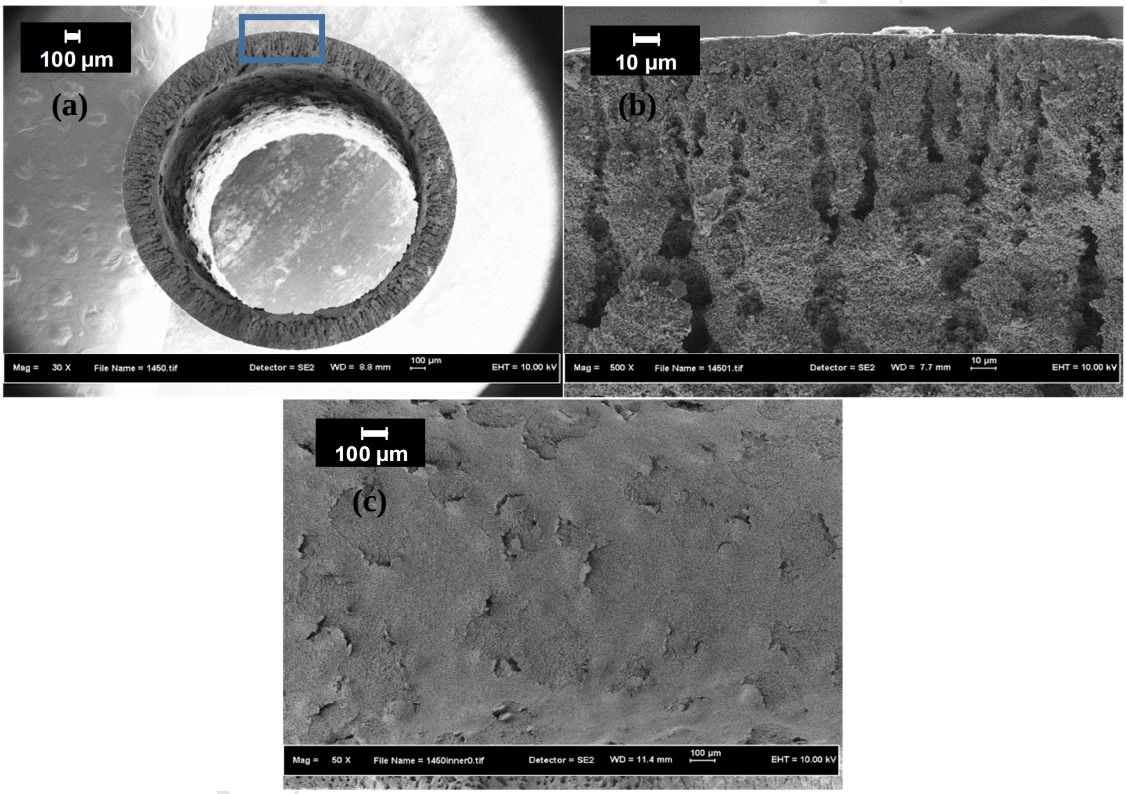

Fig. 4. SEM images of bare AHF; (a) cross-section, (b) fibre wall section and (c) inner surface

Fig. 5 shows the dispersion of MIEC perovskite oxides (LSCF and LSCNi) deposited onto alumina hollow fibre substrates through digital microscope and SEM-EDS images. From the digital microscope images shown, it can be seen that the AHF substrates were

successfully coated with the MIEC perovskite oxide as can be evidenced by a thin black layer coating on the outside of the membrane. A gradient of black colour can be seen started from the inner surface of the membrane. This indicates that the MIEC perovskite oxide sol migrates from the inner surface to the outer surface of AHF substrates due to the porous structure of AHF substrates and further concentrated on the outer wall forming a thin layer of MIEC perovskite membrane. This thin dense layer of MIEC perovskite oxide ensures that the oxygen permeation could undergo separation across the membrane wall. SEM with EDX mapping was then carried out to observe the morphology of MIEC OTM with their particular elements. All the elements were found to be homogenously deposited throughout the membrane wall similar to our previous study [38], which allow oxygen molecules undergo surface exchange reaction at the outer surface of the surface-modified membrane as well as at throughout of the membrane wall during bulk diffusion process. The amount of MIEC perovskite oxide deposited onto the bare AHF was determined from Eq. (1) and it was found that the amount of perovskite oxide deposited for LSCF-AHF and LSCNi-AHF were 0.27% and 1.03%, respectively. To further investigate the effects of MIEC perovskite oxide depositions on the AHF properties, mercury intrusion test was carried out.

LSCF-AHF LSCNi-AHF

(a) (d)

(a)

(e)

(c)

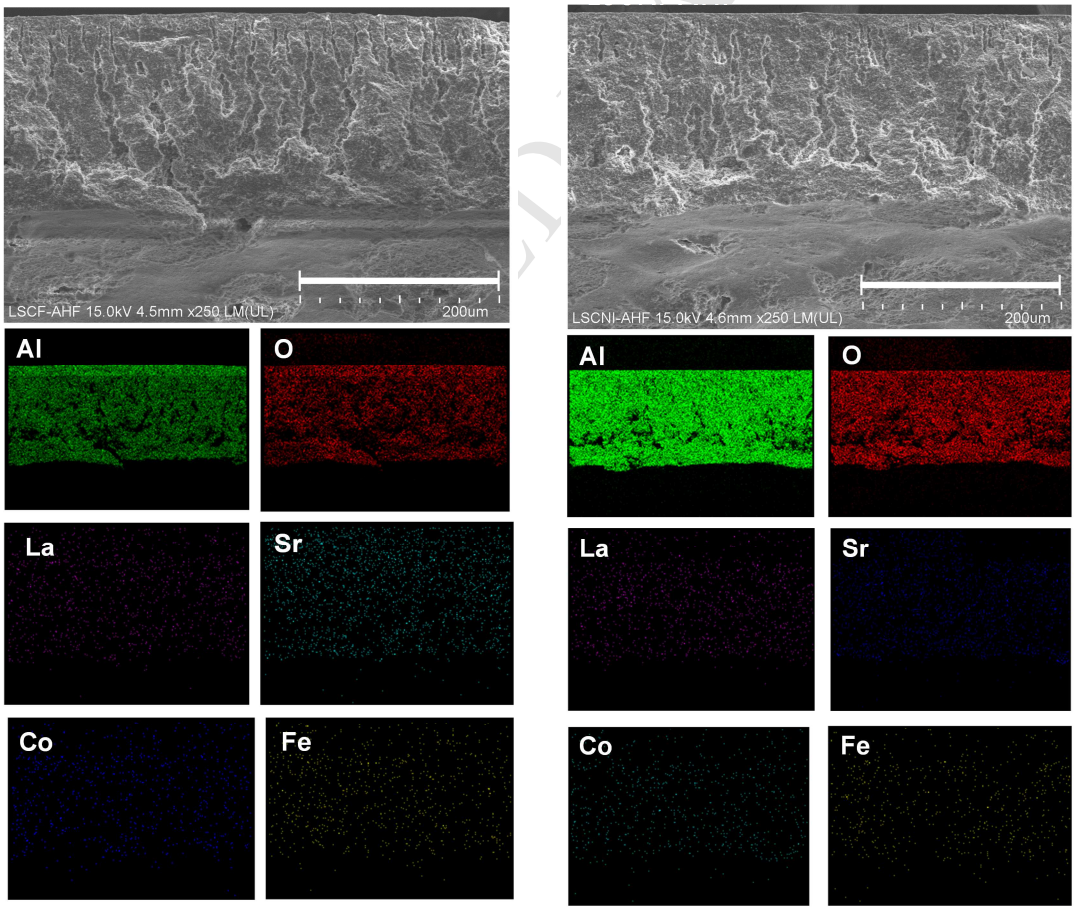

Fig. 5. SEM images and EDX mapping of bare and surface-modified AHF membranes

The porosity and pore size distribution of bare and surface-modified AHF membranes are shown in Table 1 and Fig. 6. The distribution curve shows that initially, the bare fibres possessed bigger open pores structures at around 10 to 100 µm with porosity percentage of 28.8%, thus, allowing the deposition of perovskite oxides. After the deposition, it was found that the MIEC perovskite oxides sol filled the entrance of the big pores and reduced the porosity of the AHF. Smaller pore diameter range (0.08-0.5 µm) was also observed, which might be due to the packing of MIEC inside the fingers. The LSCF-AHF and LSCNi-AHF were found to have low porosity percentage as compared to bare AHF and their distribution of pores diameter were found to be around 0.06-0.5 µm and 0.08-0.5 µm, respectively. These finding support the SEM-EDS analysis and indicates that the MIEC perovskite oxide was successfully deposited onto the AHF substrate forming a dense and gas-tight membrane that is suitable for oxygen enrichment.

Table 1. Porosity percentage of bare and surface-modified AHF membrane

Surface-modified membrane	Porosity (%)
Bare AHF	28.80
LSCF- AHF	24.69
LSCNi- AHF	24.39

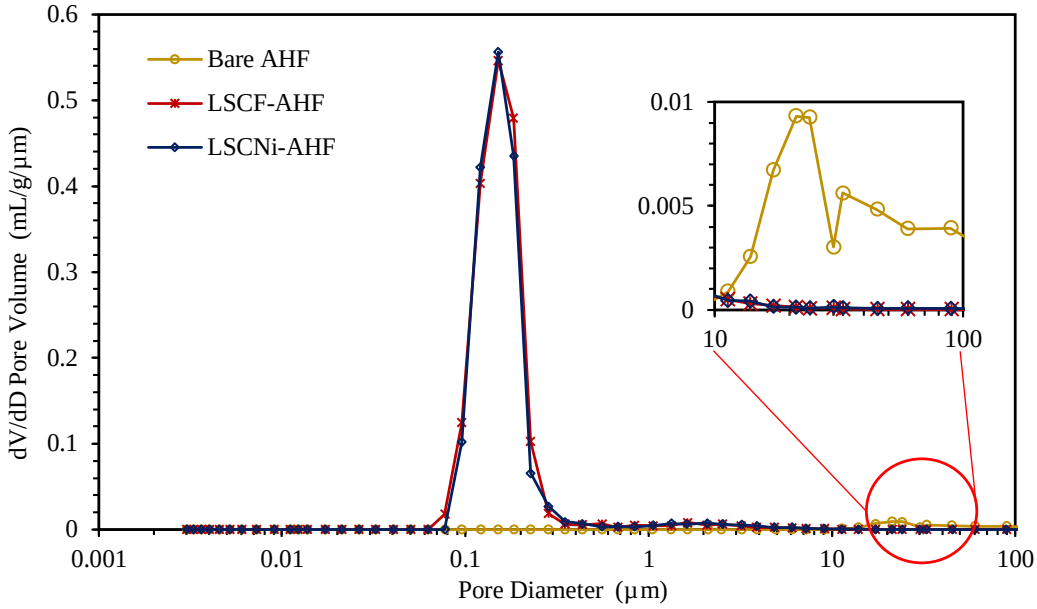

Fig. 6. Pore size distribution of bare and surface-modified AHF membrane

3.2. Oxygen permeation performance of the surface-modified AHF membranes

Fig. 7 depicts the oxygen permeation fluxes as a function of operating temperatures (700 to 950 °C) and sweep gas flowrate for fabricated LSCF-AHF and LSCNi-AHF membranes. The membranes were first subjected to gas tightness test prior to the oxygen permeation study and only gas-tight membranes were used for the study. It was observed that operating temperature plays a significant role in affecting the oxygen permeation fluxes where the O_2 flux increased with temperature for all membranes. This finding is consistent with other reported work where Tan et al. [39] demonstrate that their bare LSCF hollow fibre membrane shows an increment in O_2 permeation flux along the increasing of operating temperature (850 -1000 °C). Similar trend was also observed by Pan et al. [16] for their LSCF perovskite oxides ($SrCo_{0.9}Sc_{0.1}O_{3-\delta}$, $Ba_{0.5}Sr_{0.5}Co_{0.2}Fe_{0.8}O_{3-\delta}$, $SrCo_{0.9}Nb_{0.1}O_{3-\delta}$ and $SrCo_{0.8}Fe_{0.2}O_{3-\delta}$) coated hollow fibre within temperature range from 650-1000 °C. This indicates that higher temperature helps to enhance O_2 permeation through improvement of ionic transport and

surface exchange kinetics. According to Han et al. [32], the O_2 permeation rate is generally determined by the rate of surface exchange reaction at lower operating temperature and as the operating temperature increased, the oxygen permeation rate will be dominated by the rate of bulk diffusion rather than surface exchange reaction. This is because of the activation energy of surface exchange reaction is much smaller than that of bulk diffusion [29,32,40].

By comparison, LSCNi-AHF show higher O_2 flux than LSCF-AHF over the entire operating temperature range reaching up to 4.5 mL/cm^2.min at 950 °C and 150 mL/min of sweep gas rate. The highest O_2 flux obtained for LSCF-AHF membrane in this study was 0.55 mL/cm^2.min. All the O_2 flux observed in this work were found to be significantly higher than the range of flux value reported by Teraoka et. al [4] due to the hollow fibre configuration. In their study, the value of oxygen permeation flux for $La_{0.6}Sr_{0.4}Co_{0.8}B'_{0.2}O_3$ (B' = Cr, Mn, Fe, Co, Ni and Cu) disc membranes of 20 mm diameter and 2 mm thickness were investigated under operating temperature between 500 to 870 °C and 30 mL/min of He sweep gas flowrate. It was found that the Ni-doped perovskite oxide (LSCNi) shows significant increases in oxygen flux as compared to Fe-doped perovskite oxide (LSCF). The reported oxygen flux of LSCNi is from ~ 0.037–1.475 mL/cm^2.min while LSCF is from ~ 0.037–0.635 mL/cm^2.min between the operating temperature [4]. It can be observed that the permeation flux of LSCNi for both studies was higher as compared to LSCF due to the substitution of Ni for Co in the lattice caused the formation of vacancies of oxide ion and therefore enhance the oxygen permeability.

Besides operating temperature, O_2 permeation flux is also strongly related to oxygen partial pressure difference. Principally, the use of higher or faster argon sweep gas flowrate creates larger oxygen gradient since the oxygen partial pressure is low at permeate side of membrane [17]. The O_2 permeation flux for all the membranes was observed to consistently increase when higher sweep gas flowrates were used due to the increase of driving force for

O_2 permeation to occur associated with the O_2 partial pressure difference between feed and permeate stream. The O_2 permeation flux of LSCNi-AHF was found to increase more than 300% up to 4.47 mL/cm^2.min when the gas flowrate was increased from to 100 to 150 mL/min. Interestingly, when the LSCNi-AHF operated at 50 mL/min of sweep gas rate, the O_2 flux remained almost constant, suggesting that bulk ionic diffusion and surface exchange reaction limit the O_2 transport instead. LSCF-AHF also experienced sudden increases in O_2 flux after 850 °C when 100 mL/min of sweep gas rate was used, surpassing the O_2 permeation flux value using 150 mL/min of sweep gas rate. This might be due to the enhancement of surface reaction and the rate of oxygen ions recombining into O_2 molecules at the inner surface of hollow fibre is similar to the transport rate of O_2 in convective gas flowrate [40]. However, the effects of sweep gas flowrate will not be significant once the transport of O_2 molecules in the sweep gas flow exceeded the rate of ionic recombination or the rate of oxygen ion supply prior to ionic recombination [41].

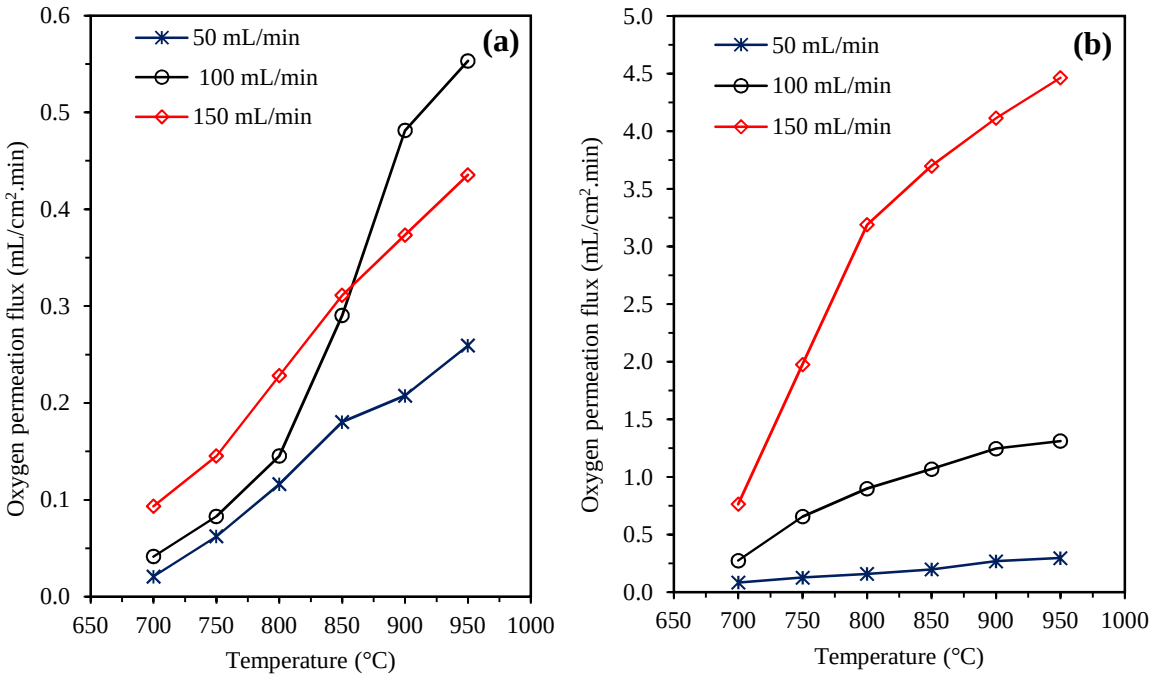

Fig. 7. Effect of sweep gas flowrates and operating temperatures on the oxygen permeation

fluxes of (a) LSCF-AHF and (b) LSCNi-AHF

4. Conclusion

This work demonstrates the possibilty of developing lanthanum-based perovskites membranes supported onto porous alumina hollow fibre (AHF) substrate for oxygen enrichment. From digital microscope and SEM-EDX analysis, a thin, dense and homogeneous layer of perovskite was deposited at the outer surface of AHF through vacuum coating. The coating of lanthanum-based perovskites onto the surface of AHF helps to improve the surface exchange reaction kinetics. A significant increase of O_2 flux at temperature above 800 °C indicates that the oxygen surface exchange reaction becomes the main factor that dominate the O_2 flux. Higher sweep gas flowrate was also found to improve the O_2 flux and LSCNi-AHF flux was observed to be significantly better than LSCF-AHF. The maximum O_2 flux value reach up to 4.47 mL/cm^2.min at 950 °C and 100 mL/min of sweep gas rate. The present work indicates a feasible method for fabricating OTM membrane using porous AHF substrates.

Acknowledgements

The authors fully acknowledged Universiti Teknologi MARA and Ministry of Higher Education (MOHE) Malaysia for the approved fund through RAGS research funding (RAGS/1/2015/TK0/UITM/02/11).

References

[1] P. Zeng, R. Ran, Z. Chen, H. Gu, Z. Shao, J.C.D. da Costa, S. Liu, Significant effects

of sintering temperature on the performance of La0.6Sr0.4Co0.2Fe0.8O3-δ oxygen selective membranes, J. Memb. Sci. 302 (2007) 171–179. doi:10.1016/j.memsci.2007.06.047.

[2] Y. Teraoka, H.M. Zhang, K. Okamoto, N. Yamazoe, Mixed ionic-electronic conductivity of La1-xSrxCo1-yFeyO3-δ perovskite-type oxides, Mater. Res. Bull. 23 (1988) 51–58. doi:10.1016/0025-5408(88)90224-3.

[3] Y. Teraoka, Y. Honbe, J. Ishii, H. Furukawa, I. Moriguchi, Catalytic effects in oxygen permeation through mixed-conductive LSCF perovskite membranes, in: Solid State Ionics, 2002: pp. 681–687. doi:10.1016/S0167-2738(02)00409-5.

[4] Y. Teraoka, T. Nobunaga, N. Yamazoe, Effect of Cation Substitution on the Oxygen Semipermeability of Perovskite-type Oxides, Chem. Lett. (1988) 503–506.

[5] J. Liu, A.C. Co, S. Paulson, V.I. Birss, Oxygen reduction at sol-gel derived La0.8Sr0.2Co 0.8Fe0.2O3 cathodes, Solid State Ionics. 177 (2006) 377–387. doi:10.1016/j.mcm.2006.01.023.

[6] L. da Conveicao, A.M. Silva, N.F.P. Ribeiro, M.M.V.M. Souza, Combustion synthesis of La0.7Sr0.3Co0.5Fe0.5O3 (LSCF) porous materials for applications as cathode in IT-SOFC, Mater. Res. Bull. 46 (2011) 308–314. doi:10.1016/j.materresbull.2010.10.009.

[7] R. Mani, R.K. Gautam, S. Banerjee, A.K. Srivastava, A. Jaiswal, M.C. Chattopadhyaya, A Study on La0.6Sr0.4Co0.3Fe0.8O3 (LSCF) Cathode Material Prepared by Gel Combustion Method for IT-SOFCs: Spectroscopic, Electrochemical and Miecrostructural Analysis, Asian J. Res. Chem. 3 (2015) 6–11. doi:10.5958/0974-4150.2015.00062.0.

[8] X. Tan, K. Li, Design of mixed conducting ceramic membranes/reactors for the partial oxidation of methane to syngas, AIChE J. 55 (2009) 2675–2685. doi:10.1002/aic.11873.

[9] J. Liu, S. Zhang, W. Wang, J. Gao, W. Liu, C. Chen, Partial oxidation of methane in a Zr0.84Y0.16O1.92–La0.8Sr0.2Cr0.5Fe0.5O3−δ hollow fiber membrane reactor targeting solid oxide fuel cell applications, J. Power Sources. 217 (2012) 287–290. doi:10.1016/j.jpowsour.2012.06.042.

[10] X. Tan, N. Liu, B. Meng, J. Sunarso, K. Zhang, S. Liu, Oxygen permeation behavior of La0.6Sr0.4Co0.8Fe0.2O3 hollow fibre membranes with highly concentrated CO2 exposure, J. Memb. Sci. 389 (2012) 216–222. doi:10.1016/j.memsci.2011.10.032.

[11] V. Middelkoop, H. Chen, B. Michielsen, M. Jacobs, G. Syvertsen-Wiig, M. Mertens, A. Buekenhoudt, F. Snijkers, Development and characterisation of dense lanthanum-based perovskite oxygen-separation capillary membranes for high-temperature applications, J. Memb. Sci. 468 (2014) 250–258. doi:10.1016/j.memsci.2014.05.032.

[12] B. Zydorczak, Z. Wu, K. Li, Fabrication of ultrathin La0.6Sr0.4Co0.2Fe0.8O3-?? hollow fibre membranes for oxygen permeation, Chem. Eng. Sci. 64 (2009) 4383–4388. doi:10.1016/j.ces.2009.07.007.

[13] D. Schlehuber, E. Wessel, L. Singheiser, T. Markus, Long-term operation of a La0.58Sr0.4Co0.2Fe0.8O3-??-membrane for oxygen separation, J. Memb. Sci. 351 (2010) 16–20. doi:10.1016/j.memsci.2010.01.022.

[14] B.-K. Lai, K. Kerman, S. Ramanathan, Nanostructured La0.6Sr0.4Co0.8Fe0.2O3/Y0.08Zr0.92O1.96/La0.6Sr0.4Co0.8Fe0.2O3 (LSCF/YSZ/LSCF) symmetric thin film solid oxide fuel cells, J. Power Sources. 196 (2011) 1826–1832. doi:10.1016/j.jpowsour.2010.09.066.

[15] Z. Wang, N. Yang, B. Meng, Preparation and oxygen permeation properties of highly asymmetric La0. 6Sr0. 4Co0. 2Fe0. 8O3− α perovskite hollow-fiber membranes, Ind. Eng. Chem. Res. 48 (2008) 510–516.

[16] H. Pan, L. Li, X. Deng, B. Meng, X. Tan, K. Li, Improvement of oxygen permeation in perovskite hollow fibre membranes by the enhanced surface exchange kinetics, J. Memb. Sci. 428 (2013) 198–204. doi:10.1016/j.memsci.2012.10.020.

[17] N. Han, S. Zhang, X. Meng, N. Yang, B. Meng, X. Tan, S. Liu, Effect of enhanced oxygen reduction activity on oxygen permeation of La0.6Sr0.4Co0.2Fe0.8O3−δ membrane decorated by K2NiF4-type oxide, J. Alloys Compd. 654 (2016) 280–289. doi:10.1016/j.jallcom.2015.09.086.

[18] D. Han, J. Sunarso, X. Tan, S. Liu, Optimizing oxygen transport through La0.6Sr0.4Co0.2Fe0.8O3−δ hollow fiber by microstructure modification and AgPt catalyst deposition.pdf, Energy and Fuels. 26 (2012) 4728–4734. doi:10.1021/ef300542e.

[19] P. Hjalmarsson, M. Søgaard, A. Hagen, M. Mogensen, Structural properties and electrochemical performance of strontium- and nickel-substituted lanthanum cobaltite, Solid State Ionics. 179 (2008) 636–646. doi:10.1016/j.ssi.2008.04.026.

[20] N.H. Sihar, A.S., Alias, N.H., Shahruddin, M.Z., Hassan, S.S.A.S., Him, N.R.N. and Othman, Sol-gel-derived perovskite-based sorbents for high-temperature air separation, J Sol-Gel Sci. 89 (2019).

[21] Kang Li, Ceramic Membranes for Separation and Reaction, 1st ed., John Wiley & Sons, Ltd, Chichester, England, 2007.

[22] B.F.K. Kingsbury, K. Li, A morphological study of ceramic hollow fibre membranes,

J. Memb. Sci. 328 (2009) 134–140. doi:10.1016/j.memsci.2008.11.050.

[23] M. Lee, B. Wang, K. Li, New designs of ceramic hollow fibres toward broadened applications, J. Memb. Sci. 503 (2016) 48–58. doi:10.1016/j.memsci.2015.12.047.

[24] M. Lee, Z. Wu, R. Wang, K. Li, Micro-structured alumina hollow fibre membranes - Potential applications in wastewater treatment, J. Memb. Sci. 461 (2014) 39–48. doi:10.1016/j.memsci.2014.02.044.

[25] M. Lee, B. Wang, Z. Wu, K. Li, Formation of micro-channels in ceramic membranes - Spatial structure, simulation, and potential use in water treatment, J. Memb. Sci. 483 (2015) 1–14. doi:10.1016/j.memsci.2015.02.023.

[26] X. Tan, N. Liu, B. Meng, S. Liu, Morphology control of the perovskite hollow fibre membranes for oxygen separation using different bore fluids, J. Memb. Sci. 378 (2011) 308–318. doi:10.1016/j.memsci.2011.05.012.

[27] N. Liu, X. Tan, B. Meng, S. Liu, Honeycomb-structured perovskite hollow fibre membranes with ultra-thin densified layer for oxygen separation, Sep. Purif. Technol. 80 (2011) 396–401. doi:10.1016/j.seppur.2011.04.014.

[28] P. Monash, G. Pugazhenthi, P. Saravanan, Various fabrication methods of porous ceramic supports for membrane applications, Rev. Chem. Eng. 29 (2013) 357–383. doi:10.1515/revce-2013-0006.

[29] W. Jin, S. Li, P. Huang, N. Xu, J. Shi, Fabrication of La0.2Sr0.8Co0.8Fe0.2O(3-δ) mesoporous membranes on porous supports from polymeric precursors, J. Memb. Sci. 170 (2000) 9–17. doi:10.1016/S0376-7388(99)00352-X.

[30] C. Yacou, J. Sunarso, C.X.C. Lin, S. Smart, S. Liu, J.C. Diniz da Costa, Palladium surface modified La0.6Sr0.4Co0.2Fe0.8O3-?? hollow fibres for oxygen separation, J.

Memb. Sci. 380 (2011) 223–231. doi:10.1016/j.memsci.2011.07.008.

[31] A. Leo, S. Smart, S. Liu, J.C. Diniz da Costa, High performance perovskite hollow fibres for oxygen separation, J. Memb. Sci. 368 (2011) 64–68. doi:10.1016/j.memsci.2010.11.002.

[32] D. Han, J. Wu, Z. Yan, K. Zhang, J. Liu, S. Liu, La0.6Sr0.4Co0.2Fe0.8O3−δ hollow fibre membrane performance improvement by coating of Ba0.5Sr0.5Co0.9Nb0.1O3−δ porous layer, RSC Adv. 4 (2014) 19999. doi:10.1039/c4ra00704b.

[33] N.H. Othman, M.Z. Shahruddin, A.S. Sihar, Z. Wu, K. Li, In-Situ Catalytic Surface Modification of Micro-Structured Vacuum-Assisted technique, MATEC Web Conf. 69. 05002 (2016) 1–6. doi:10.1051/matecconf/20166.

[34] N.H. Othman, Z. Wu, K. Li, An oxygen permeable membrane microreactor with an in-situ deposited Bi1.5Y0.3Sm0.2O3-δ catalyst for oxidative coupling of methane, J. Memb. Sci. 488 (2015) 182–193. doi:10.1016/j.memsci.2015.04.027.

[35] N.H. Othman, M.Z. Shahruddin, A.S. Sihar, Z. Wu, K. Li, In-Situ catalytic surface modification of micro-structured La0.6Sr0.4Co0.2Fe0.8O3-δ (LSCF) Oxygen Permeable Membrane Using Vacuum-Assisted technique, in: MATEC Web Conf., 2016. doi:10.1051/matecconf/20166905002.

[36] A.S. Sihar, M.Z. Shahruddin, N.H. Alias, A.N. Che Abdul Rahim, N.H. Othman, M.A. Rahman, Catalytic Surface Modification of Alumina Membrane For Oxygen, J. Teknol. 2 (2017) 29–34.

[37] X. Tan, Z. Wang, H. Liu, S. Liu, Enhancement of oxygen permeation through La0.6Sr0.4Co0.2Fe0.8O3-[delta] hollow fibre membranes by surface modifications, J. Memb. Sci. 324 (2008) 128–135. doi:10.1016/j.memsci.2008.07.008.

[38] A.S. Sihar, M.F. Mohd Rodzi, A.N. Che Abd Rahim, M.Z. Shahrudin, N.H. Alias, N.H. Othman, Preparation of Mixed Ionic Electronic Conducting (MIEC) Membrane Supported on Al2O3 Substrate : Effects of Substrate Morphology, IOP Conf. Ser. Mater. Sci. Eng. 358 (2018) 1–6. doi:10.1088/1757-899X/358/1/012057.

[39] X. Tan, Z. Wang, H. Liu, S. Liu, Enhancement of oxygen permeation through La0.6Sr0.4Co0.2Fe0.8O3-?? hollow fibre membranes by surface modifications, J. Memb. Sci. 324 (2008) 128–135. doi:10.1016/j.memsci.2008.07.008.

[40] C. Yacou, J. Sunarso, C.X.C. Lin, S. Smart, S. Liu, J.C. Diniz da Costa, Palladium surface modified La0.6Sr0.4Co0.2Fe0.8O3-δ hollow fibres for oxygen separation, J. Memb. Sci. 380 (2011) 223–231. doi:10.1016/j.memsci.2011.07.008.

[41] J. Sunarso, S. Liu, Y.S. Lin, J.C. Diniz Da Costa, High performance BaBiScCo hollow fibre membranes for oxygen transport, Energy Environ. Sci. 4 (2011) 2516–2519. doi:10.1039/c1ee01180d.